High Frequency Induced Enhancements of the Incoherent Scatter Spectrum at Arecibo, 2

IVAN J. KANTOR[1]

Department of Space Science, Rice University, Houston, Texas 77001

When the ionospheric F region is illuminated with a strong O mode HF radio wave, excitations of longitudinal plasma and acoustic waves are observed by 430-MHz radar scattering. The frequency structure of the excited waves and their variability with local parameters, time, and space are described. The observations are interpreted in terms of parametric instability theory. The spectra of the observed features and the correlation of their amplitudes are shown. The upshifted and downshifted plasma lines exhibit some marked asymmetries. Absolute as well as relative amplitudes of the enhancement are presented.

A new frontier in ionospheric physics has been opened with the experiment of modifying the ionosphere with intense HF radio waves. The opportunity is available to the researcher to control some of the conditions of the experiment in addition to observing the natural variation of the ionospheric plasma. This ability should contribute to the understanding of the thermal processes, the dynamics and the ion chemistry of the upper atmosphere, and the instabilities in plasmas. The use of radio waves [*Utlaut and Cohen*, 1971] that interact with the ionosphere is very attractive because of the repeatability, controllability, reversibility, and freedom from material contamination. The work described below emphasizes the use of the ionosphere as a plasma for selected controlled experiments.

A radio wave propagating in the ionosphere loses energy to the medium by particle collisions, thereby increasing the electron temperature, or by decaying into other modes, e.g., plasma waves (parametric instabilities). Any of these phenomena can be appreciable only with high incident power densities. For HF radio waves (the system limits are 4–11 MHz, but the frequency allocation limits work to 5.1 MHz and above) observations have been concentrated in the F region mainly near the 200- to 300-km altitude range, where the transmitted frequency matches the local plasma frequency and where the deviative absorption is large. This work is in contrast to previous experiments by *Showen* [1972] that used a 40-MHz heater to alter the electron temperature in the D and E regions.

The idea of modifying the F layer with powerful HF waves originated almost a decade ago with *Farley* [1963] and *Gurevich* [1967]. To date, the modification experiments have produced several interesting results, many of which were not widely anticipated. One particularly interesting case, anticipated by F. W. Perkins (private communication, 1970), is the observation of plasma waves induced by strong HF radio waves associated with plasma instabilities, which are the subject of this paper.

The data presented here were obtained at the Arecibo Observatory by using the incoherent backscatter facility. Previous results from the modification experiments at Arecibo are given by *Gordon et al.* [1971] and *Carlson et al.* [1972]. The present paper updates the article by *Carlson et al.* [1972], using more recent data and techniques.

[1] Now at Instituto de Pesquisas Espaciais, CP515, S. J. Campos, Sao Paulo, Brazil.

PLASMA LINES

The power spectrum of the incoherent backscatter radar has two main features [*Salpeter*, 1961]: the ion component and the plasma line component (Figure 1). The ion component is a pair of lines broadened by Landau damping straddling the radar frequency (430 MHz) with a width of the order of the ion acoustic frequency. Most scatter experiments have been concerned with the ion component of the spectrum [e.g., *Evans*, 1969; *Gordon*, 1967].

The plasma lines correspond to a pair of narrow lines located at 430 MHz $\pm f_r$, where the resonance frequency f_r is given by [*Yngvesson and Perkins*, 1968]

$$f_r^2 = f_p^2 + \frac{12KT_e}{\lambda^2 m_e} + f_c^2 \sin^2\theta$$

where f_p is the plasma frequency, K the Boltzmann constant, T_e the electron temperature, λ the wavelength, m_e the electron mass, f_c the gyrofrequency, and θ the angle between the wave vector and the magnetic field. The observed plasma lines are produced by scattering from weakly damped longitudinal plasma oscillations with frequency f_r, wavelength $\lambda/2$ and phase velocity $v_{ph} = f_r\lambda/2$.

Naturally occurring plasma lines were first observed by *Perkins et al.* [1965] during the daytime. The intensity of the daytime plasma lines is enhanced by the photoelectron fluxes, in agreement with the nonequilibrium theory of *Perkins and Salpeter* [1965]. Daytime plasma lines are regularly observed at Arecibo [*Yngvesson and Perkins*, 1968; *Wickwar*, 1971; *Wickwar and Carlson*, 1973]. The intensity is typically a noise temperature of a few tens of degrees.

At night, without the photoelectron excitation, the intensity of the plasma lines is much lower (typically a factor of 100), and they have only recently been observed (H. C. Carlson, private communication, 1972). The night observations are due only to the thermal electron distribution, and the power at each line relative to the ion power is given by [*Perkins et al.*, 1965] $\sigma_{PL} = \sigma_{ion}/2\alpha^3$, where $\alpha = 1/kD$,

$$\sigma_{ion} \simeq \sigma_e/[1 + (T_e/T_i)] \qquad \alpha \gg 1$$

and D is the Debye wavelength.

The presence of the HF radio wave can by a parametric process [*Perkins and Kaw*, 1971] induce plasma oscillations

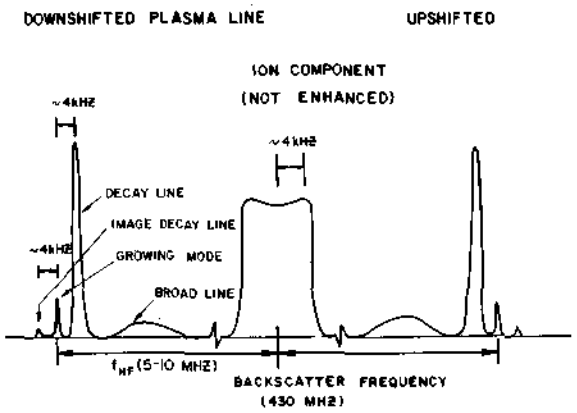

Fig. 1. Schematic backscatter spectrum during ionospheric heating.

much stronger than those produced by the photoelectrons. This HF enhancement was first observed at Arecibo in January 1971 [*Carlson et al.*, 1972]. Whereas the photoelectrons enhance the plasma line intensities by a factor of the order of 100 over the ambient thermal level, the HF radio waves were observed to produce enhancement factors exceeding 10^5. When the frequency of the propagating electromagnetic wave is close to the local plasma frequency of the medium, some instabilities can be created. The propagating electromagnetic wave, referred to as the pump or heater wave, modulates some of the parameters of the plasma that couple different modes of oscillation in the plasma. In physical terms, the parametric instability can be understood in the following way [*Goldman*, 1966]. The radio wave at the pump frequency f_{HF} modulates the plasma dielectric constant at this frequency. A wave propagating in the same plasma at a frequency f will also modulate the dielectric constant, producing polarization currents at the frequencies $f \pm f_{HF}$, which in turn act as sources for new excitations at $f \pm 2f_{HF}$ and f. This feedback process leads to amplification of these modes of oscillation. The longitudinal modes of oscillation are the only important ones to be considered for the observations because they are the only ones to be observed as radar backscatter from the density fluctuations that they produce. The decay instability was predicted by *DuBois and Goldman* [1965, 1967], and its importance for the heating experiment was presented by *Perkins and Kaw* [1971]. The nonlinear calculation of the spectra is given by *DuBois and Goldman* [1972*a*, *b*] and *Valeo et al.* [1972]. The linear calculation applicable to observations at a specific radar k (the practical case in question here) has been given by *Hagfors and Gieraltowski* [1972].

Experimental Conditions

The experiment involves sending high-power HF radio waves into the ionosphere, while incoherent backscatter observations monitor the ionospheric parameters. Ionosondes and photometers are also used.

The HF transmitter used at Arecibo delivers up to 160 kW of power at discrete frequencies between 5.1 and 10.8 MHz into a log periodic antenna at the focus of a 300-m reflector. It is possible to transmit in CW and pulsed mode in both right- and left-hand circular polarization. The Arecibo backscatter facility [*Gordon and LaLonde*, 1961] makes use of a 2.5-MW peak power (150-kW maximum average power), 430-MHz transmitter feeding into a 300-m-diameter dish. The half-power beam width of the resultant diagnostic beam is $\frac{1}{6}°$.

Basically, the plasma line data are obtained in the following way (Figure 2). The 430-MHz transmitter sends a short pulse. The plasma waves in the ionosphere produce scattering of this pulse at frequencies displaced from 430 MHz by the frequency of the plasma waves. These scattered waves are received and amplified through a system of amplifiers, local oscillators, and filters. The signal is digitized and recorded on tape. It can be further Fourier-analyzed, giving a power spectrum, or can be used as a power profile of the plasma waves.

This paper covers HF enhanced plasma line data obtained from May 1971 to October 1972 as they have been analyzed to date. It is not possible to present all of them, but a general description and a presentation of a few examples are given.

Spectra of the Plasma Line

Figure 1 shows a schematic backscatter plasma line that contains all of the features normally observed. There are no standard names for those features, but in anticipation of the physical interpretation, the nomenclature in this paper will be the following: (1) the 'growing mode' or line for the enhancement displaced from the backscatter frequency (430 MHz) by the frequency of the heating transmitter, (2) the 'decay line' for the enhancement displaced by an ion acoustic frequency (approximately 3½ kHz) toward the ion component from the growing mode frequency, (3) the 'broad line' for one or more enhancements (widths of the order of 10 kHz) displaced toward the ion component from the decay line, (4) the 'image decay line' for the enhancement displaced by an ion acoustic frequency away from both the growing mode frequency and the backscatter frequency, and (5) the 'plasma line' for the whole spectrum in the vicinity of 430 MHz + f_{HF} or 430 MHz − f_{HF}.

Usually, the most prominent feature is the decay line. Figure 3 shows calibrated plasma lines upshifted and downshifted. For the Arecibo radar system sensitivity, the peak amplitude of the decay line can reach 10^6 °K (in a 1-kHz band), and in general the upshifted and downshifted decay lines are asymmetric in amplitude. In contrast, the photo-

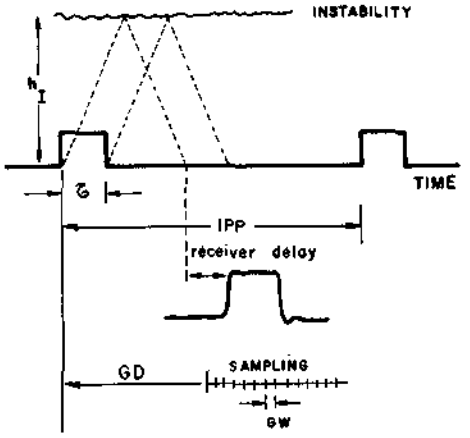

Fig. 2. High frequency enhanced plasma line signal.

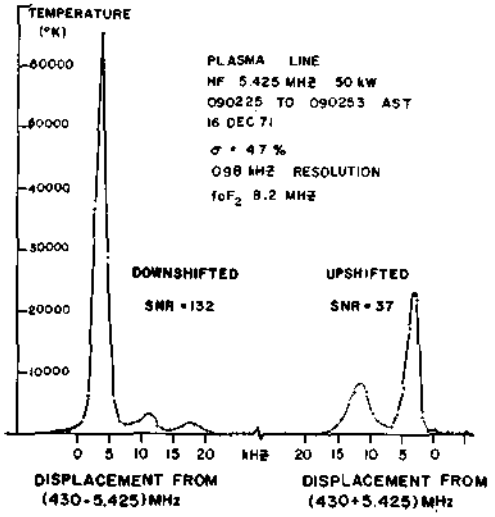

Fig. 3. Upshifted and downshifted plasma line, calibrated in antenna temperature. Displacement is positive toward the 430-MHz backscatter frequency.

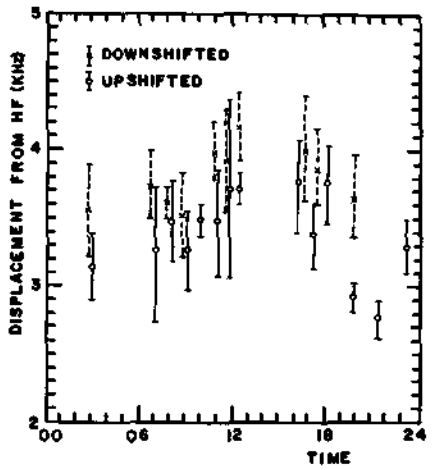

Fig. 4. Diurnal variation of the decay line displacement from the HF frequency. Contains data from May 1971 to March 1972. The bars represent the range of all available data for 1-hour intervals.

electron enhanced plasma line usually has an intensity of the order of 10^3 °K. The HF induced plasma lines are normally so intense as to be seen visually on the oscilloscope (the peak snr of the decay line at times exceeding 10^5). The frequency of the peak of the enhancements is of interest. For the full set of analyzed observations (over 3000), the peak of the decay line ranges from a 2.6- to a 4.4-kHz displacement from 430 MHz $\pm$ f_{HF}, the positive sign being toward the ion component. The standard deviation of each measurement is 0.1 kHz. With this choice of sign, the upshifted and downshifted decay lines have positive signs. The parametric decay instability produces an enhancement displaced by the ion acoustic frequency [e.g., *Valeo et al.*, 1972], which is in the range of the observed decay lines; thus their name is derived from this instability. For Arecibo parameters and O^+, the ion acoustic frequency is given by

$$f_a = 6.54 \times 10^{-2}(T_e + 3T_i)^{1/2} \qquad (1)$$

in kilohertz, where T_e and T_i are the electron and ion temperatures in degrees Kelvin. The ion acoustic frequency ranges from 3.5 to 6 kHz. Appreciable fractions of NO^+ and O_2^+ below 250 km lead to somewhat lower ion acoustic frequencies.

When all the frequency displacement data are plotted against the time of day, the following picture emerges (Figure 4):

1. The frequency displacement from the HF is different for the upshifted and downshifted decay lines, and the difference is almost constant throughout the day, averaging 0.4 $\pm$ 0.1 kHz. The upshifted decay line is on the average always below the downshifted decay line.

2. The displacement is higher during the day than during the night, following an approximately diurnal electron temperature dependence. The decay line displacement is related to the electron and ion temperature (1) by $\Delta f \propto (T_e + 3T_i)^{1/2}$. When $T_e = T_i$ is assumed at night and the displacements during the day (Δf_D) and the night (Δf_N) are known, the ratio T_e/T_i for daytime hours can be calculated:

$$T_e/T_i = 4(\Delta f_D/\Delta f_N)^2 - 3$$

When $\Delta f_D = 3.8$ kHz (4.1 kHz) and $\Delta f_N = 3.3$ kHz (3.6 kHz) are substituted for the upshifted (downshifted) decay line, the daytime ratio T_e/T_i is calculated to be 2.3 (2.2), which is very reasonable for the F layer altitudes in question.

When the smearing from some decay line data of 0.5-kHz resolution is removed when the heater frequency is 8.195 MHz by the application of the function $\sin x/x$, the half-power bandwidth is 1.2 kHz.

Parametric instability theory predicts the existence of the purely growing instability, displaced by the pump frequency f_{HF} from the backscatter frequency (430 MHz). Figure 5 presents two observed spectra of plasma lines illustrating the growing instability. The spectra were obtained with different pump powers. Note that the ratio between the peak of the decay line and the peak of the growing line is the same for the two HF power levels. The observed peak of the growing line for all available data ranges from a factor of ½ to zero times the peak amplitude of the plasma line. This factor remains constant for time periods of hours. The growing mode, however, is not usually seen.

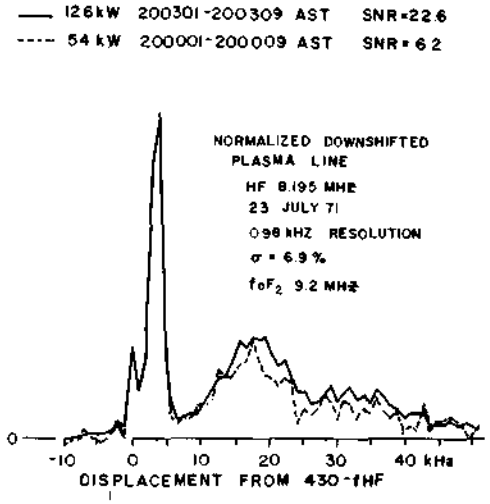

Fig. 5. Normalized downshifted plasma line for different HF powers. Note that although the peak signals have very different snr, the shapes are quite similar.

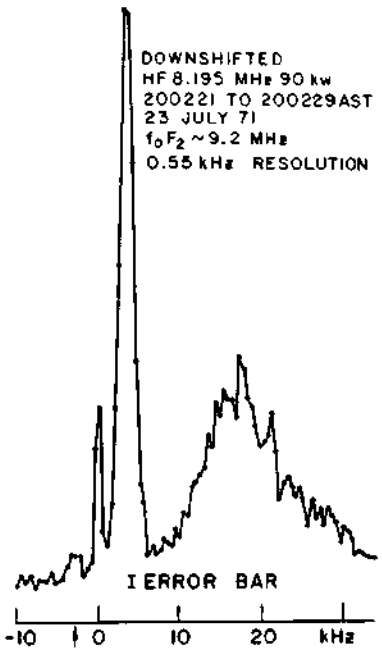

Fig. 6. Spectrum of plasma line. Arrow indicates image decay line.

In Figures 3 and 5 a wide enhancement or a series of wide enhancements is observed beyond 10 kHz from the pump toward the ion line. They have recently been interpreted by *Kruer and Valeo* [1972] and *Kuo and Fejer* [1972]. The peak signal of the broad line is usually smaller than the peak of the decay line, but the power in the broad line can be twice the power in the decay line. The broad line is usually present when there is a decay line. The equivalent width of the broad line (power divided by peak signal) ranges from 2 to 10 kHz, and the peak is 7–20 kHz from the pump. Sometimes a series of enhancements is observed, in which case they may be close to some harmonics of the displacement of the decay line from the pump (Figure 3) or they may have broader structures (Figure 5). Very rarely a very wide enhancement (20 kHz) is present together with all the other features, centered in the broad line range. The power of the decay line is found to be on the average 60%, ranging from 20 to 100% of the total power of all the features. The peak power at the broad line divided by the peak power of the decay line ranges from

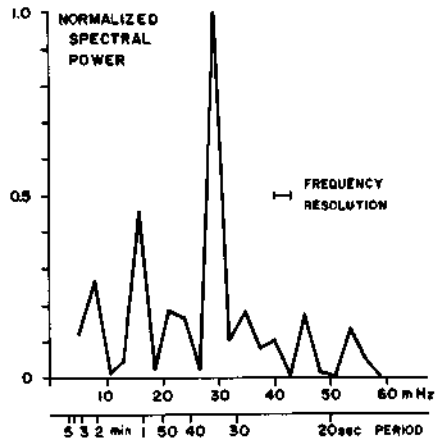

Fig. 8. Power spectrum of time fluctuation of upshifted decay line in Figure 5. Sharp peak is 35-s period.

0.04 to 0.4 for the upshifted plasma line and from 0.08 to 0.45 for the downshifted data reduced to date (approximately 53 spectra). This ratio for the upshifted line is approximately equal to that for the simultaneously measured downshifted line in the 0.2–0.45 range.

Another weak enhancement is occasionally present, displaced from the pump frequency away from 430 MHz by the ion acoustic frequency. It can be thought of as an image of the decay line about the pump frequency. An arrow on the frequency scale in Figure 6 indicates this feature.

TIME DEPENDENCE

There are fluctuations of the enhanced plasma line intensity over a wide range of time scales. On time scales of hours, the observed severe decrease of intensity near midday in the 5- to 6-MHz range of HF frequencies appears to be due to F_1 region absorption. On time scales of tens of minutes, one sunset run showed [*Kantor and Meltz*, 1973] severe regular periodic fading of the plasma line intensity, which can be explained in terms of the height of the instability sliding through consecutive maximums and minimums of the (Airy function) interference field strength near the reflection height. The rate of fading from one minimum to the next depends on the rate of change of the local density gradient as f_0F_2 approaches the heater frequency f_{HF}. The envelope of the maximums decreases as f_0F_2 approaches f_{HF} (within the last percent).

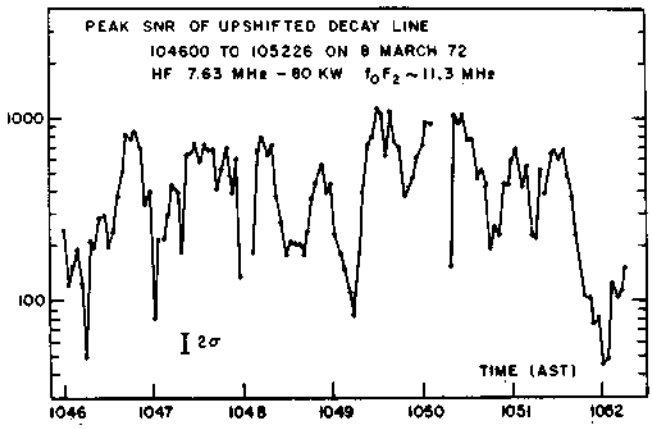

Fig. 7. Time fluctuation of upshifted decay line. Samples are taken every 3 s. Amplitude scale is logarithmic.

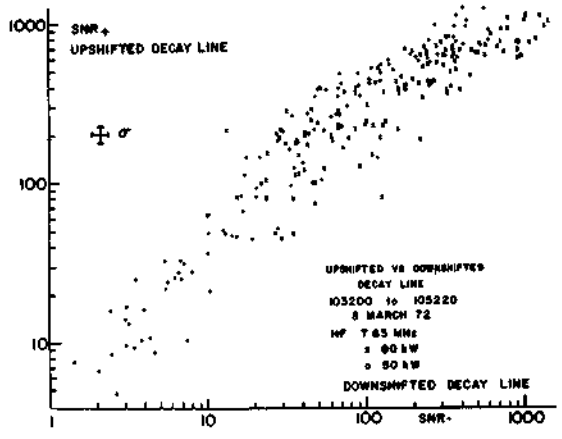

Fig. 9. Upshifted versus downshifted peak snr of decay line during natural amplitude fading at two different heater powers.

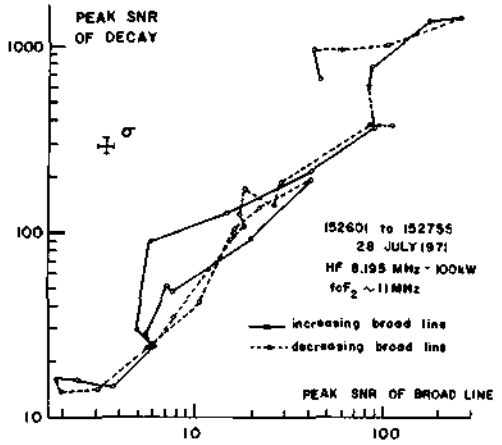

Fig. 10. Peak snr of the peak of the decay line versus peak snr of the peak of the broad line at constant P_{HF}.

The plasma line intensity is observed to vary by almost 1 order of magnitude about a mean value at times. The spectral analysis of the variation of the peak intensity shows sharp resonances. Figure 7 shows the time variation of the peak intensity, and Figure 8 shows the spectral analysis of it. The period of oscillation of the main spectral component from all available data ranges from 35 s to 3 min.

By plotting the amplitude of the upshifted line versus that of the downshifted line (Figure 9), a relationship between them is observed. The circles represent amplitudes when the transmitter power P_{HF} is 50 kW ($\sim$20 μW/m^2) (when about 2 dB of D and E region absorption is assumed [*Davies*, 1965]), and the crosses amplitudes when P_{HF} = 80 kW ($\sim$32 μW/m^2). Figure 9 shows some interesting points.

The natural fluctuations of the plasma line amplitude for the two power densities overlap over a decade. In a separate experiment, varying P_{HF} over values of power different from 50 and 80 kW (not shown) also overlaps with the upshifted-downshifted dependence of Figure 9. This behavior suggests that the time fluctuations of the plasma line are due solely to variations of the electric field at the height of the plasma line.

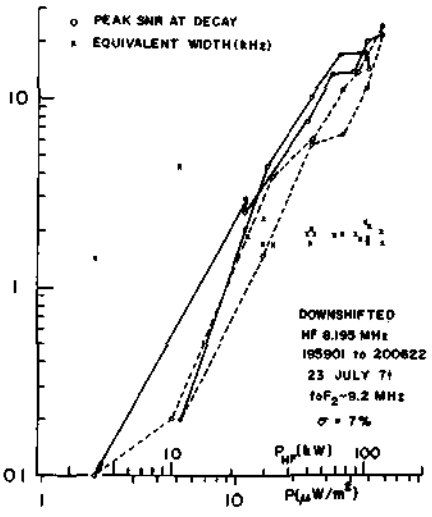

Fig. 11. Peak snr of decay line versus HF power P_{HF}. Circles represent data points. Solid line connects points where P_{HF} increases, and dashes points where P_{HF} decreases. Crosses give the equivalent thickness of the decay line. Data are taken every 20 s.

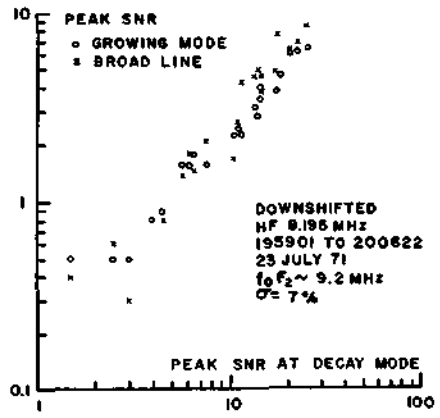

Fig. 12. Peak snr of growing mode (open circles) and broad line (crosses) as a function of peak snr of decay mode corresponding to different HF powers. Log-log scale. Linear fit gives a 1.2 power law.

The upshifted-downshifted dependence indicates two linear regions: (snr)$_-$ < 100 when $S_- \propto S_+^{1.00\pm0.25}$ and (snr)$_-$ > 100 when $S_- \propto S_+^{2.4\pm0.3}$. The low-amplitude region indicates that upshifted and downshifted amplitudes are varying linearly, but above approximately snr $\sim$ 70 the downshifted amplitude grows faster than the upshifted amplitude.

Not only are the upshifted and downshifted decay lines closely related, but so are the broad line and the decay line (Figure 10). The peak amplitudes of the decay line and the broad line are approximately proportional.

More detailed results about fluctuations of the plasma line amplitude will be presented in a separate article. The diurnal variation of the plasma line power cannot yet be established.

Power Dependence

The dependence of the plasma line on the transmitted power is difficult to determine because of the natural fluctuation of the plasma line. On occasion, the amplitude of the plasma line is stable enough that a measurement of the power dependence is possible. Only the decay line intensities are shown as a function of P_{HF}, and other features are shown as a function of the decay line intensities. The data scatter is less this way, and all features are probably related to the local electric field. Figures 3, 5, and 10–13 are

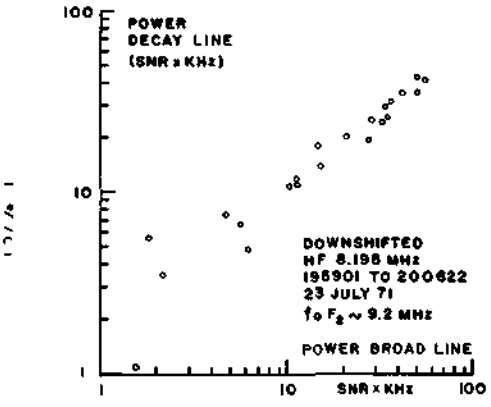

Fig. 13. Power in decay line versus power in broad line, each point corresponding to a different HF power. Log-log scale. Linear fit gives an 0.8 power law.

from the same experiment, so that one can relate their results.

The peak snr and the power in the decay line follow a power dependence with the HF power in Figure 11 with exponent ~1.5. In different experiments the exponent ranges from 1.2 to 4. Figure 11 also shows the equivalent width, which is 1.9 kHz with little dependence on P_{HF}, so that the power of the plasma line has the same power dependence as the peak snr. Solid lines connect data where P_{HF} increases with time, and dashed lines connect data for the opposite case. A hysteresis is usually observed. No sharp break in the power dependence is found; thus no change from a linear to an unstable regime is observed; thus the threshold does not seem to be observed because it is either much below or much above the incident power density. Along the P_{HF} scale, a power density scale is given that assumes average conditions with no D and E region absorption. Note that they are proportional, so that the power dependence of the decay line on the local power density has the same exponent as that for P_{HF}.

When the decay line varies, owing to a change in P_{HF}, all the features follow proportionally (Figure 5). The spectra are normalized to the peak of the decay line. The amplitudes of the growing mode and the broad line change very little, and the general shape is unchanged. Figure 12 shows the peak snr of the growing mode and of the broad line as a function of the peak snr of the decay line. Figure 13 shows the power of the broad line as a function of the power of the decay line. The power is estimated as the area under the line minus a pedestal. The features are almost linearly dependent. The exponent of the variation of the features with the decay line is 1.2, which is similar to those measured in our experiments, where it ranges from 1.1 to 1.5 for downshifted plasma lines and from 1.8 to 2.4 for upshifted plasma lines. The fact that the growing mode and the broad line have the same amplitude is a coincidence.

Figure 14 shows that the equivalent width of the broad line (power/peak representing the width of a rectangle of the same height and area as the broad line) is little dependent on power. The error increases for lower powers.

There is not very much change of the decay line displacement with P_{HF}. Observations and theoretical prediction show that it is less than 2% (50 Hz) up to 120 kW [*Kantor*, 1972].

COMPARISON OF UPSHIFTED AND DOWNSHIFTED PLASMA LINES

The upshifted plasma line in general differs in shape from the downshifted line. Present theories are unable to explain a difference between the upshifted and the downshifted lines. This section summarizes the differences.

1. The shape of the plasma line is in general different. In Figure 3 there are three maximums in the downshifted spectrum, whereas there are only two in the upshifted spectrum.

2. The amplitude of the signal is in general different (Figure 3) even correcting for the difference in antenna gain.

3. The frequency displacement of the decay line of the downshifted line is in general ~½ kHz larger than that for the upshifted line (Figure 4). Plasma movement is insufficient to account for this difference.

4. The upshifted and downshifted plasma line peak amplitudes are within a factor of 3 of each other. The relation is illustrated in Figure 9, so that the two plasma lines vary together generally but not in detail.

5. The decay of upshifted and downshifted plasma lines is different. On one daytime measurement taken at 16h 29m 00s AST for an HF of 8.18 MHz, the plasma line decay was 814 μs for the upshifted line and 610 μs for the downshifted line. This difference is not inconsistent with theory and can be interpreted by the difference of flux between upgoing and downgoing photoelectron fluxes.

6. The ratio of the broad line peak to decay line peak is different when this same ratio is less than 0.2, as was mentioned previously.

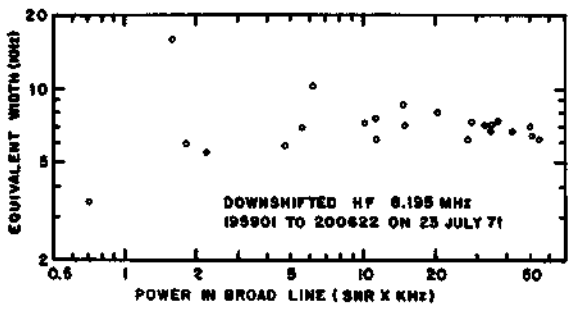

Fig. 14. Equivalent width of the broad line as a function of its power. Approximately 7 kHz independent of power.

RISE AND DECAY TIMES

Enhancement rise times after HF turn-on have been found to be of the order of tens of milliseconds and show a ringing of the plasma line not present on the HF transmitted pulse. The period of the ringing was about 8 ms on two measurements spaced by 20 min in time (R. L. Showen, private communication, 1972). This ringing may be the same found by *Kruer and Valeo* [1972].

Decay times of the plasma line intensity after HF turn-off are about 0.3–1 ms, consistent with the linear theory [*Yngvesson and Perkins*, 1968] for the frequency range studied. They are primarily due to wave damping by photoelectrons and are shortest for waves going in the direction of the largest flux. This finding has obvious application to photoelectron flux studies. At night the decay rates are slower by a factor of roughly 2–10, again consistent with the linear theory, primarily owing to electron ion collisions. No significant nonlinear damping has yet been detected. More complete results will be presented in a later article.

ION LINE

Figure 15 (G. Ioannides, private communication, 1972) shows a typical backscatter power profile of the ion line taken with the Barker decoded signal. The height resolution is 900 m. The HF transmitter was delivering 54 kW at 5.425 MHz, and the figure shows a spike in the backscatter signal. A similar power profile taken minutes later but with the Barker signal at the plasma line frequency (not shown) has a similar spike in the same altitude box, indicating that the ion and the plasma line enhancements come from the same altitudes (193 km in Figure 15) within the 900-m resolution. The layer thickness has to be less than 900 m, since the spike appears in only one range box.

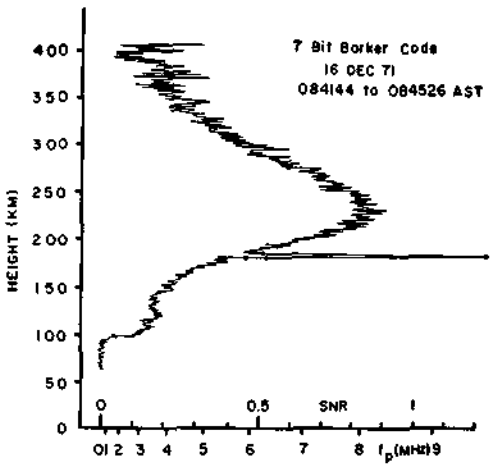

Fig. 15. Barker code profile showing an enhanced ion line. The profile has been corrected for radar range. The individual points are separated by 0.9 km (baud length, 6 μs). Plasma frequency scale is only indicative because the Barker data do not have T_e/T_i correction (G. Ioannides, private communication, 1972) ($P_{HF} = 54$ kW, $f_{HF} = 5.425$ MHz).

The enhancement of the ion line due to the HF radio wave predicted by instability theory [*Dubois and Goldman*, 1965] is a pair of lines displaced from the center frequency by the same amount as the plasma line is displaced from the HF, owing to the decay instability, and an enhancement at the center frequency corresponding to the growing mode.

The ion component shows a highly variable amount of enhancement. One 600-m-resolution observation of the HF enhanced ion autocorrelation function showed (H. C. Carlson, private communication, 1972) an enhanced echo strength of about 10^2 and an enhanced correlation beyond the first zero crossing, a decay of subsequent maximums and minimums being indicative of peaking of the ion spectra at the ion acoustic frequency. Substantially higher quality ion component autocorrelation data have since been gathered, showing enhancement factors of about 2–5 (with 2.7-km resolution) (C. Zamlutti and T. Hagfors, private communication, 1972). These data are of sufficient quality to permit estimates of the width of the apparent spikes on the ion spectral wings.

Figure 16 shows a plot of the ion enhancement peaks versus the upshifted plasma line peak. The dashed line represents a square law dependence: ion enhancement = 0.04(plasma line)^2. The data seem to follow closely the square law. Below the threshold for instability the ion component is hardly affected [*Hagfors and Gieraltowski*, 1972]; this may suggest that the ion enhancement is above threshold.

Spatial Extent of the Layer Producing the Plasma Line

Observations to measure the height thickness of the layer associated with the enhancement in the plasma line yielded only an upper boundary of 300 m [*Kantor*, 1972]. Note that the observations represent a fixed **k** vector, which means that the region affected by the instability is much larger.

The plasma line power can be mapped with respect to azimuth and zenith angles by moving the diagnostic 430-MHz beam. Figure 17 shows a portion of a zenith angle map of a plasma line observed through a 100-kHz bandwidth filter. The antenna scanned 1°/min along the magnetic meridian, and the zenith angle is larger than 4°, owing to physical blocking by the HF antenna. Data are taken each 14 min of arc (14 s apart) while the antenna moves. Data are not yet available out of the magnetic meridian. Two sets of data are taken to estimate the temporal variations.

In Figure 17 there are no detected enhanced plasma lines for larger zenith angles out to 13° except for the solid line at the south. By accident, the HF transmitter turned off at $\theta = 9°$ for the south solid line data, not making clear where the plasma line cutoff is in general, but twice on other occasions it did not exceed 9°. The half-power width of the HF beam (~10°) and the plasma lines can be observed over almost 20°, centered close to 1°N zenith angle.

The HF antenna half-power beam width is 8.5° at 6.79 MHz, and the angle between nulls is 21°.

Owing to the presence of the magnetic field, the reflection of the ordinary rays takes place at the same height for all the zenith angles $\theta < \theta_{cr}$. This cusp is called 'Spitze,' and θ_{cr} is given by [e.g., *Ginzburg*, 1970]

$$\sin \theta_{cr} = \sin \theta/(1 + f_{HF}/f_c)^{1/2}$$

θ being the angle between the magnetic field and the vertical. With no magnetic field, Snell's law gives an $H \sin^2 \theta$ dependence of the height of the wave reflection.

Since the unstable region is typically 1.2 km below the vertical incidence reflection point, it means that, without the

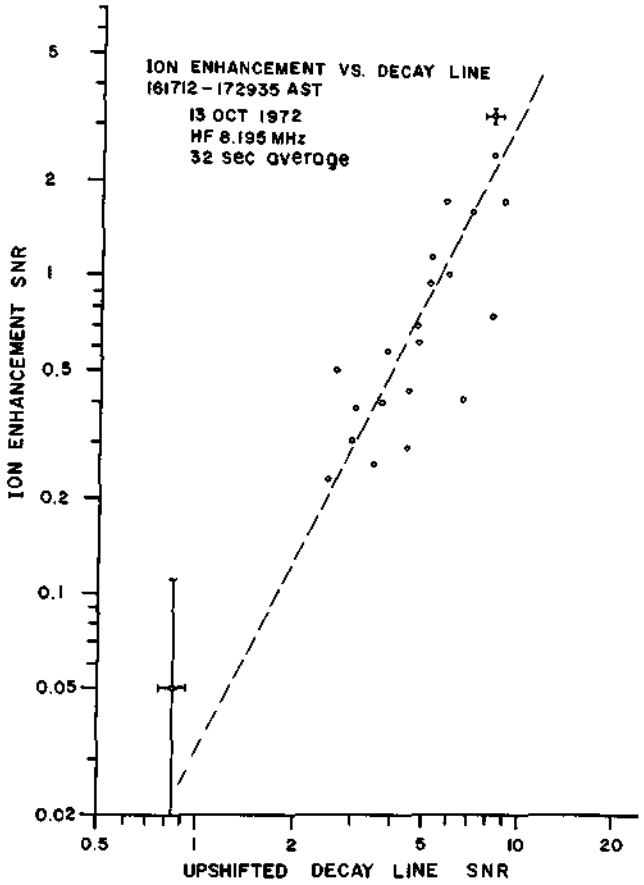

Fig. 16. Peak power of the ion enhancement versus upshifted plasma line peak from Barker decoder. Dashed line represents quadratic power dependence.

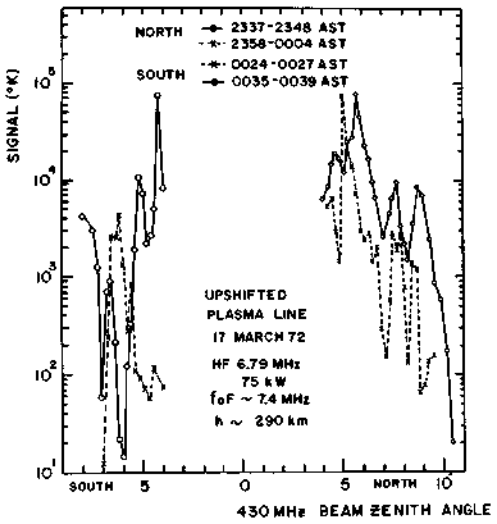

Fig. 17. Plasma line power of upshifted plasma line as a function of zenith angle. Dashed and solid lines represent data taken at different times.

magnetic field, waves departing from the antenna at more than a typical 12° zenith angle would be reflected before reaching the height where the instabilities are observed.

One infers that the observed gross zenith angle dependence of the plasma line is due to the antenna pattern, since the critical angle is greater than 16° at the heater frequency.

X Mode Enhancements

All plasma line enhancements observed were excited by an O mode wave. *Carlson et al.* [1972] noted the absence of the X mode enhancements. Experiments were repeated, but the results are inconclusive as of this writing. The usual parametric instabilities cannot be excited by the X mode because the wave will be reflected before reaching an altitude where the HF is nearly matched to the local plasma frequency [*Fejer*, 1971], but Bernstein modes could be excited [*Fejer and Leer*, 1972].

Cross Section

The cross section of the plasma line enhancement is of interest for comparison with theoretical predictions. The easiest way to measure is by comparison with a known cross section, in this case, the ion line. Figure 18 shows the raw data spectrum after filter shape correction of both the upshifted and downshifted plasma lines and the ion line. The incoherent backscatter snr is given by [e.g., *Evans*, 1969]

$$\text{snr} = (0.76P_T/8\pi h^2 KB)/(A\sigma\ \Delta h/T)$$

where

- P_T backscatter transmitted power;
- h range of the reflection;
- K Boltzmann constant;
- B bandwidth of the signal;
- A area of the plasma;
- σ backscatter cross section;
- Δh height interval where backscattering is taking place;
- T system temperature.

When the ion signal is compared with the plasma line signal, some of the parameters can be canceled. For the ion, $\Delta h = \tau c/2$, where τ is the backscatter pulse length (1200 μs) and c the speed of light, making it 180 km. With this pulse length the ion enhancement, if present, is smeared in altitude, and the power is less than 1% of the power of the unenhanced ion component [*Kantor*, 1972]. When an index I denotes the ordinary ion data and an asterisk the plasma line enhanced data,

$$\sigma^*\ \Delta h^*/\sigma_I = \Delta h_I \theta^*/\theta_I$$

where $\theta = \text{snr} \cdot T/A$ is a signal temperature corrected for the antenna gain. In Figure 18, when the area of the decay

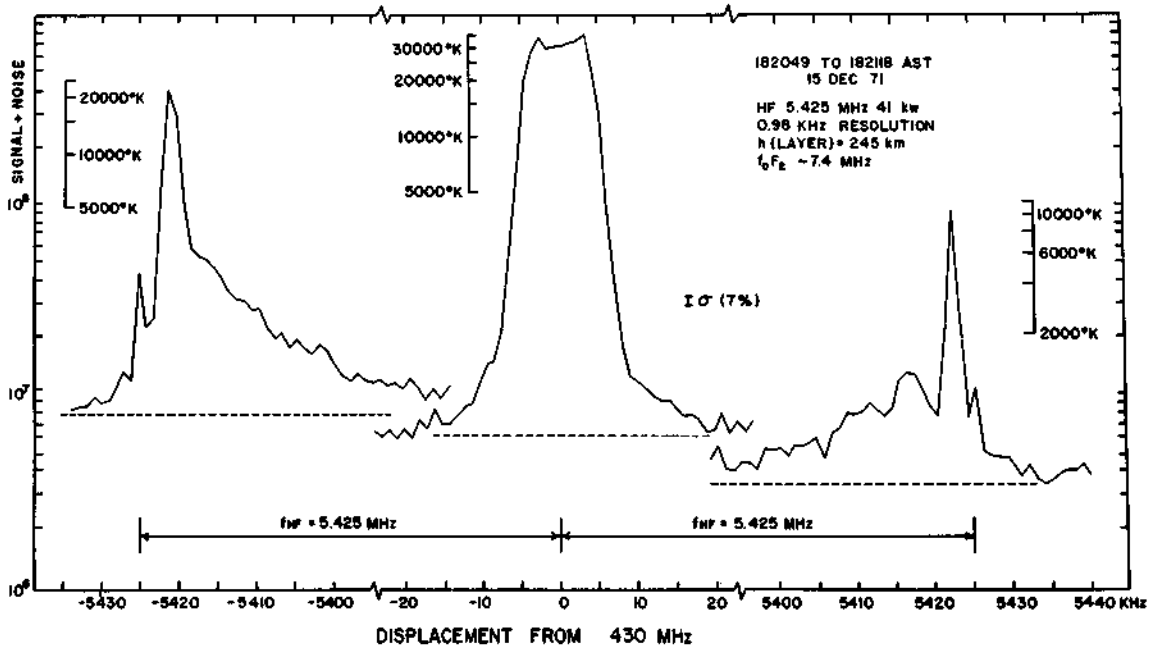

Fig. 18. Raw data spectrum after filter shape correction of upshifted and downshifted enhanced plasma line. Center spectrum is the ion component taken simultaneously for comparison. Dashed base below spectra gives the noise level.

TABLE 1. Values Calculated by Dividing the Area of the Decay Line Spike and the Ion Line in Figure 18 by the Noise Level

	Downshifted	Ion Component	Upshifted
snr	93	1139	30
T, °K	444	277	460
A/A(ion)	0.8035	1	0.5649
θ, °K	51,317	315,503	24,340
$\sigma^* \Delta h^*/\sigma_I$, km	29		14

line spike and the ion line are taken and are divided by the noise level (indicated by the horizontal dashed lines), the values in Table 1 can be calculated.

If the height interval Δh^* is the same for upshifted and downshifted plasma lines, then the downshifted cross section is 2.1 times the upshifted. As the data indicate $\Delta h^* < 0.3$ km, then the downshifted (upshifted) cross section is more than 97 (42) times the ion component cross section.

By means of equation 12 from *Harker* [1972], the following expression is found (in his notation):

$$\frac{\sigma^* \Delta h^*}{\sigma_I} = 16\pi^2 H E^2 \left(\frac{k}{k_D}\right)^2 \left(\frac{\mu^2}{1 - \mu^2}\right)$$

for the threshold region above. For the subthreshold condition, the same expression applies if $(1 - E^2\mu^4)^{1/2}$ is substituted for $1 - \mu^2$ in the denominator. The HF transmitted 41 kW at 5.425 MHz. The enhancement was observed at 245 km. At this height, the electron density scale height was 26 km, and the electron and ion temperatures were 1040° and 900°K, respectively. Using these parameters and those given by *Harker* [1972] yields $E^2 = 1.0$ and $\sigma^* \Delta h^*/\sigma_I = 26$. This value agrees well with the data.

CONCLUSIONS

The decay line, the growing mode, and image of the decay line are identified and associated with the components of parametric instabilities.

Asymmetries between the upshifted and the downshifted plasma lines are indicated, but no interpretation is found.

The decay time constant of the plasma line is consistent with that given by the electron-ion collision frequency and the photoelectron Landau damping of the linear theory.

The sweeping of the height of the parametric instability through the structure of the HF electric field near the reflection height as the f_0F_2 fall through the heater frequency produces oscillations of the amplitude of the plasma line.

At other times, the plasma line is observed to oscillate, apparently owing to fluctuations of the electric field at the height of the instability.

The peak amplitude of the growing mode and the broad line is approximately proportional to the peak amplitude of the decay line.

The gross zenith dependence of the plasma line is determined by the HF antenna pattern in the case of Arecibo. The Spitze phenomenon is shown to be important in the interpretation of zenith angle data.

Acknowledgments. I would like to thank my advisor, W. E. Gordon, for his constant care and excellent guidance throughout all the stages of this work. This work would not have been possible without the mutual collaboration in running the experiments and reducing the data by the 'heating team,' composed of W. E. Gordon, H. C. Carlson, L. A. Dias, V. Wickwar, R. L. Showen, J. Rowe, R. Behnke, and F. Schwab. I am indebted to F. Perkins for his theoretical discussions and advice, to H. C. Carlson for long and fruitful discussions, to T. Hagfors for his constant encouragement, and to D. B. Campbell and J. Rankin for some useful discussions on spectral analysis. I wish to thank P. Watkins and F. Schwab for doing some of the computer work and G. Ioannides for furnishing some of the results from the Barker decoder. I wish to thank the staff of the Arecibo Observatory for their cooperation and support throughout the experiments.

This work is supported in part by the Institute of Space Research, INPE (Brazil), where the author is a staff member, and in part by National Science Foundation grant GA-17452. The National Astronomy and Ionospheric Center (Arecibo Observatory) is supported by the National Science Foundation and operated by Cornell University. Support for the heating experiments was provided by the Advanced Research Projects Agency under contracts F30602-70-C-0187, F-30602-71-C-0155, and F30602-C-0278 and monitored by the Air Force Systems Command, Rome Air Development Center.

* * *

The Editor thanks R. Cohen and J. A. Fejer for their assistance in evaluating this paper.

REFERENCES

Carlson, H. C., W. E. Gordon, and R. L. Showen, High frequency induced enhancements of the incoherent scatter spectrum at Arecibo, *J. Geophys. Res., 77*, 1242–1250, 1972.

Davies, K., Ionospheric radio propagation, *NBS 80*, pp. 217–256, U.S. Dep. of Commer., Washington, D.C., 1965.

DuBois, D. F., and M. V. Goldman, Radiation induced instability of electron plasma oscillations, *Phys. Rev. Lett., 14*, 544–546, 1965.

DuBois, D. F., and M. V. Goldman, Parametrically excited plasma fluctuations, *Phys. Rev., 164*, 207–222, 1967.

DuBois, D. F., and M. V. Goldman, Nonlinear saturation of parametric instability: Basic theory and application to the ionosphere, *Phys. Fluids, 15*, 919–927, 1972*a*.

DuBois, D. F., and M. V. Goldman, Spectrum and anomalous resistivity for the saturated parametric instability, *Phys. Rev. Lett., 28*, 218–221, 1972*b*.

Evans, J. V., Theory and practice of ionosphere study by Thomson scatter radar, *Proc. IEEE, 57*, 496–530, 1969.

Farley, D. T., Jr., Artificial heating of the electrons in the *F* region of the ionosphere, *J. Geophys. Res., 68*, 401–413, 1963.

Fejer, J. A., Effect of ionospheric heating by radio waves on the absorption of probing waves of different polarization, *J. Geophys. Res., 76*, 285–286, 1971.

Fejer, J. A., and E. Leer, Excitation of parametric instabilities by radio waves in the ionosphere, *Radio Sci., 7*, 481–491, 1972.

Ginzburg, V. L., *The Propagation of Electromagnetic Waves in Plasmas*, 2nd ed., p. 399, Pergamon, New York, 1970.

Goldman, M. V., Parametric plasmon-photon interaction, 1, 2, *Ann. Phys., 38*, 95–116, 117–169, 1966.

Gordon, W. E., *F* region and magnetosphere, Backscatter results, *Rev. Geophys. Space Phys., 5*, 191–205, 1967.

Gordon, W. E., and L. M. LaLonde, The design and capabilities of an ionospheric radar probe, *IRE Trans. Antennas Propagat., 9*, 17–22, 1961.

Gordon, W. E., R. Showen, and H. C. Carlson, Ionospheric heating at Arecibo: First tests, *J. Geophys. Res., 76*, 7808–7813, 1971.

Gurevich, A. V., Radiowave effect on the ionosphere in the *F*-layer region, *Geomagn. Aeron., 7*, 291–297, 1967.

Hagfors, T., and G. F. Gieraltowski, Stable electron density fluctuations in a plasma in the presence of a high-frequency electric field, *J. Geophys. Res., 77*, 6791–6803, 1972.

Harker, K. J., Induced enhancement of the plasma line in the backscatter spectrum by ionospheric heating, *J. Geophys. Res., 77*, 6904–6906, 1972.

Kantor, I. J., Enhanced plasma lines excited by HF waves, Ph.D. dissertation, Rice Univ., Houston, Tex., 1972.

Kantor, I. J., and G. Meltz, Ionospheric heating at Arecibo: HF electric field structure at reflection, submitted for publication, 1973.

Kruer, W. L., and E. J. Valeo, Nonlinear evolution of the decay instability in a plasma with comparable electron and ion temperatures. *Rep. MATT-919,* Princeton Univ. Plasma Phys. Lab., Princeton, N.J., Aug. 1972.

Kuo, Y.-Y., and J. A. Fejer, Spectral line structures of saturated parametric instabilities, *Phys. Rev. Lett., 29,* 1667–1670, 1972.

Perkins, F. W., and P. K. Kaw, On the role of plasma instabilities in ionospheric heating by radio waves, *J. Geophys. Res., 76,* 282–284, 1971.

Perkins, F. W., and E. E. Salpeter, Enhancement of plasma density fluctuations by nonthermal electrons, *Phys. Rev., Sect. A, 139,* 55–62, 1965.

Perkins, F. W., E. E. Salpeter, and K. O. Yngvesson, Incoherent scatter from plasma oscillations in the ionosphere, *Phys. Rev. Lett., 14,* 579–581, 1965.

Salpeter, E. E., Plasma density fluctuations in a magnetic field. *Phys. Rev., 122,* 1663–1674, 1961.

Showen, R. L., Artificial heating of the lower ionosphere, *J. Geophys. Res., 77,* 1923–1933, 1972.

Utlaut, W. F., and R. Cohen, Modifying the ionosphere with intense radio waves, *Science, 174,* 245–254, 1971.

Valeo, E., C. Oberman, and F. Perkins, Saturation of the decay instability for comparable electronic and ion temperatures, *Phys. Rev. Lett., 28,* 340–343, 1972.

Wickwar, V. B., Photoelectrons from the magnetic conjugate point studied by means of the 6300 predawn enhancement and the plasma line enhancement, Ph.D. dissertation, Rice Univ., Houston, Tex., 1971.

Wickwar, V. B., and H. C. Carlson, Application of the plasma line technique to photoelectron studies, submitted for publication, 1973.

Yngvesson, K. O., and F. W. Perkins, Radar Thomson scatter studies of photoelectrons in the ionosphere and Landau damping, *J. Geophys. Res., 73,* 97–110, 1968.

(Received April 5, 1973;
accepted September 4, 1973.)